

Fabrication of solution-processed hydrogenated amorphous silicon single-junction solar cells

Takashi Masuda, Naoya Sotani, Hiroki Hamada, Yasuo Matsuki, and Tatsuya Shimoda

Citation: *Appl. Phys. Lett.* **100**, 253908 (2012); doi: 10.1063/1.4730614

View online: <http://dx.doi.org/10.1063/1.4730614>

View Table of Contents: <http://apl.aip.org/resource/1/APPLAB/v100/i25>

Published by the [American Institute of Physics](http://www.aip.org).

Related Articles

Millisecond annealing for advanced doping of dirty-silicon solar cells

J. Appl. Phys. **111**, 123104 (2012)

Exploration of nano-element array architectures for substrate solar cells using an a-Si:H absorber

J. Appl. Phys. **111**, 123103 (2012)

Combined plasmonic and dielectric rear reflectors for enhanced photocurrent in solar cells

Appl. Phys. Lett. **100**, 243903 (2012)

On-line thermal dependence study of the main solar cell electrical photoconversion parameters using low thermal emission lamps

Rev. Sci. Instrum. **83**, 063105 (2012)

Amorphous/crystalline silicon heterojunction solar cells via remote inductively coupled plasma processing

Appl. Phys. Lett. **100**, 233902 (2012)

Additional information on *Appl. Phys. Lett.*

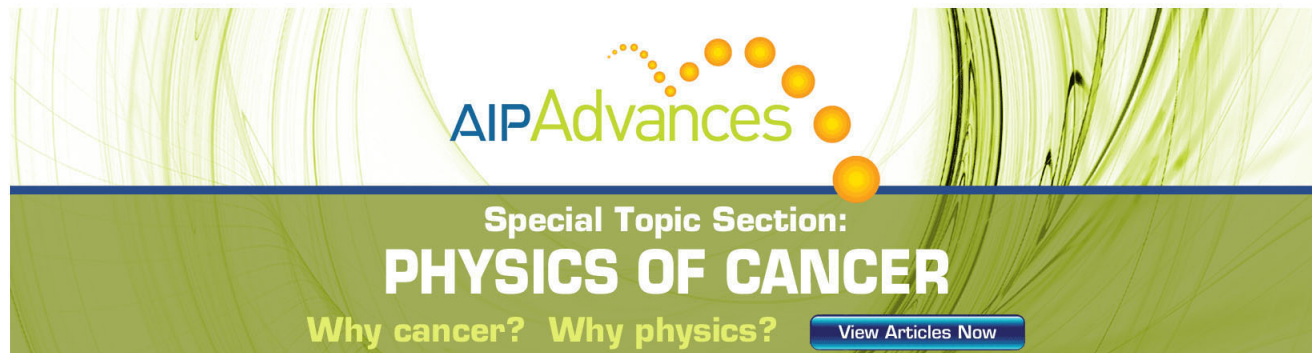
Journal Homepage: <http://apl.aip.org/>

Journal Information: http://apl.aip.org/about/about_the_journal

Top downloads: http://apl.aip.org/features/most_downloaded

Information for Authors: <http://apl.aip.org/authors>

ADVERTISEMENT

The advertisement features a green and yellow abstract background with flowing lines. At the top, the 'AIP Advances' logo is shown, with 'AIP' in blue and 'Advances' in green, accompanied by a series of orange dots of varying sizes. Below the logo, the text 'Special Topic Section:' is in white, followed by 'PHYSICS OF CANCER' in large, bold, white capital letters. At the bottom, the phrase 'Why cancer? Why physics?' is written in yellow, and a blue button with the text 'View Articles Now' is positioned to the right.

AIP Advances

Special Topic Section:
PHYSICS OF CANCER

Why cancer? Why physics? [View Articles Now](#)

Fabrication of solution-processed hydrogenated amorphous silicon single-junction solar cells

Takashi Masuda,^{1,a)} Naoya Sotani,^{2,b)} Hiroki Hamada,^{2,c)} Yasuo Matsuki,^{1,3} and Tatsuya Shimoda^{1,4}

¹Japan Science and Technology Agency, ERATO, Shimoda Nano-Liquid Process Project, 2-13 Asahidai, Nomi, Ishikawa 923-1211, Japan

²Solar Energy Research Center, SANYO Electric Co., 180 Ohmori, Anpachi-cho, Anpachi-Gun, Gifu 503-0195, Japan

³Yokkaichi Research Center, JSR Corporation, 100 Kawajiri-cho, Yokkaichi, Mie 510-8552, Japan

⁴School of Materials Science, Japan Advanced Institute of Science and Technology, 1-1 Asahidai, Nomi, Ishikawa 923-1292, Japan

(Received 7 March 2012; accepted 7 June 2012; published online 22 June 2012)

Hydrogenated amorphous silicon solar cells were fabricated using solution-based processes. All silicon layers of the p-i-n junction were stacked by a spin-cast method using doped and non-doped polydihydrosilane solutions. Further, a hydrogen-radical treatment under vacuum conditions was employed to reduce spin density in the silicon films. Following this treatment, the electric properties of the silicon films were improved, and the power conversion efficiency of the solar cells was also increased from 0.01% to 0.30%–0.51% under the AM-1.5G (100 mW/cm²) illumination conditions.

© 2012 American Institute of Physics. [<http://dx.doi.org/10.1063/1.4730614>]

Solution-based processes for the fabrication of electronic devices have attracted attention because of their wide application and cost-effectiveness in comparison with conventional vacuum-based processes. In particular, solution-processed semiconducting materials are very useful in the development of next-generation electronic devices such as large-area flexible solar cells and thin-film transistors. Recent advances in solar cells using solution processes have principally found application in organic semiconductors,¹ some of which have a power conversion efficiency comparable with that of a hydrogenated amorphous silicon (a-Si:H) solar cell. However, issues of reliability have remained. The stable and highly efficient operation of solution-processed solar cells based on copper indium gallium selenide has also been reported.² Although this class of materials appears to be an alternative to silicon, the supply of rare metals is problematic. Therefore, research efforts have concentrated on developing solution-processed silicon solar cells in an efficient way. In this study, we report the fabrication of a-Si:H solar cells using solution-based processes except for metal electrodes and modification treatment to silicon layers. All silicon layers of the p-i-n junction were prepared by a spin-cast method, and the quality of the silicon layers was improved by a hydrogen-radical treatment under vacuum condition. This latter procedure was applied because our solution-processed a-Si:H film required a help of a vacuum process to achieve a good-quality silicon film for applying to solar cell devices. We have also demonstrated the effectiveness of the hydrogen-radical treatment.

We have previously synthesised a silicon precursor solution consisting of polydihydrosilane $-(\text{SiH}_2)_n-$, cyclopentasilane (CPS: Si_5H_{10}), and organic solvent and

have fabricated a solution-processed polysilicon thin-film transistor with the help of laser annealing.³ We have also investigated the surface tension of CPS, the characteristics of polydihydrosilane solution, and the stability of polydihydrosilane film.^{4–6} Solution-processed a-Si:H films can be prepared by the pyrolysis of polydihydrosilane at an appropriate pyrolysis temperature (T_p). For the fabrication of the p-i-n junction structure, we prepared doped and non-doped a-Si:H films on the basis of similar techniques used for solution-processed silicon films.³ To fabricate the p-type a-Si:H (p-Si) film, the p-type polydihydrosilane was synthesised by photo-induced ring-opening polymerisation of CPS, in which decaborane was dissolved at 80 °C. The dopant concentration in the film was adjusted by changing the quantity of decaborane in the CPS. The wavelength, intensity, and irradiation time for the ultraviolet (UV) light-induced reaction were 365 nm, 15 mW/cm², and 10–60 min, respectively. The resultant polymer was dissolved in distilled CPS solvent. This p-type polydihydrosilane solution was spin-coated on the quartz substrate at 2000 rpm for 30 s and pyrolysed at $T_p = 390$ °C for 30 min in a sealed chamber to prevent desorption of the decaborane. For the n-type a-Si:H (n-Si) film, the n-type polydihydrosilane was prepared in a similar way to that employed for the p-type film.⁷ Instead of decaborane, we used white phosphorus obtained by cracking red phosphorus. The wavelength, intensity, and irradiation time were 405 nm, 300 mW/cm², and 5–120 min, respectively. Distilled cyclooctane was used as a solvent for the n-type polydihydrosilane solution. The solution was spin-coated on the substrate and pyrolysed at $T_p = 390$ °C for 30 min on a hot plate. For the intrinsic a-Si:H (i-Si) film, the non-doped polydihydrosilane was also prepared without dopant. The wavelength, intensity, and irradiation time were 365 nm, 15 mW/cm², and 10 min, respectively. Distilled cyclooctane was used as a solvent for non-doped polydihydrosilane solution. The i-Si film was fabricated with similar way to that of n-Si film.

^{a)}Author to whom correspondence should be addressed. Electronic mail: mtakashi@jaist.ac.jp.

^{b)}Solar Business Unit, Energy Company, SANYO Electric Co., Ltd., Energy Company of Panasonic Group.

^{c)}Next-Generation Energy Device Development Center, Panasonic Corp.

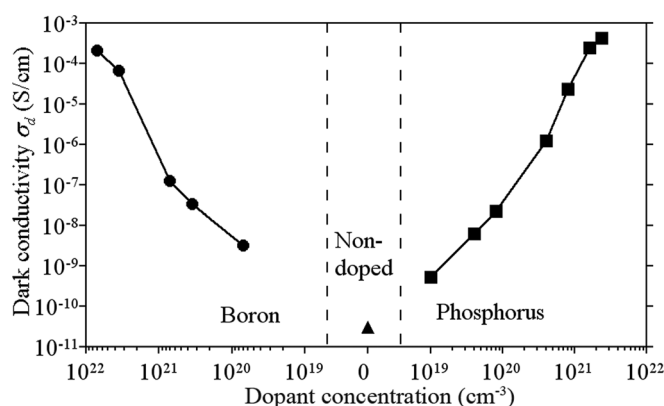


FIG. 1. Dark conductivity (σ_d) vs. dopant concentration for p- and n-Si films at 25 °C. The σ_d of the i-Si film is also plotted. The σ_d of p-, i-, and n-type films are plotted by closed circles, triangle, and squares, respectively.

To confirm the formation of a-Si:H films, we employed Raman scattering techniques. It was found that the Raman spectrum of phonon bands from the p-, i-, and n-Si films was almost identical to that of vacuum-processed a-Si:H films, and thus these doped films were concluded to be in the amorphous state. The dark conductivity (σ_d) at 25 °C for the p- and n-Si films with the thickness of 50 nm is plotted as a function of boron or phosphorus concentration in Figure 1, where σ_d for the i-Si film is also given. The dopant concentration was measured by secondary ion mass spectrometry (SIMS). The σ_d of both the p- and n-Si films show a significant increase with dopant concentration. These results suggest that boron and phosphorus in the doped a-Si:H films act as acceptors and donors, respectively. The conductivity of our solution-processed doped a-Si:H films without the hydrogen-radical treatment is smaller by one to three orders of magnitude than that of device-grade vacuum-processed a-Si:H films.⁸ The maximum concentration of boron and phosphorus is limited by the solubility of the decaborane and white phosphorus in CPS, which were 7×10^{21} and $2 \times 10^{21} \text{ cm}^{-3}$, respectively.

To apply the solution-processed doped and non-doped a-Si:H films to solar cell devices, the film quality was improved using the hydrogen-radical treatment via hot-wire chemical vapour deposition. The apparatus used was nearly identical to that described in the literature.⁹ A tungsten wire with a diameter of 0.5 mm and a length of 100 cm was used as a catalyser and heated at 1850 °C. Hydrogen gas (99.9999% purity) was introduced into the chamber at a flow

rate of 15 sccm for 15 min. The chamber pressure and the substrate temperature were maintained at 0.2 Pa and 200 °C, respectively.

The properties of the i-, p-, and n-Si films with and without the hydrogen-radical treatment are listed in Table I. Typical properties of vacuum-processed i-Si films are also listed as a reference. The hydrogen content, optical gap, and spin density were measured by SIMS, UV-visible transmittance and reflectance spectroscopy, and electron spin resonance, respectively. The conductivity was measured on a coplanar configuration of 250 μm gap width, using aluminum contacts for samples. An increase in hydrogen content and drastic reduction of spin densities by the hydrogen-radical treatment were observed in all of the silicon films. The depth profile by SIMS measurement (data not shown) showed that the hydrogen was increased not only surface but entire film. It indicates that the hydrogen radical diffused in the film and terminated the defect. As a result, with this treatment, a large increase in photoconductivity (σ_p) and a decrease in σ_d in the i-Si film were achieved, while the σ_d values of the p- and n-Si films were increased. These properties of resultant a-Si:H films showed comparable value to device-grade vacuum-processed ones.¹⁰ These improvements may be attributed to the reduction of spin densities.

Figure 2 shows a schematic structure of the solution-processed a-Si:H p-i-n single-junction solar cell. The solar cells were fabricated according to the following four steps: (1) a flat ZnO layer with a sheet resistivity of 100 Ω/sq and a thickness of 200 nm was sputtered onto the glass substrate with an area of $5 \times 5 \text{ cm}^2$, (2) the p-Si layer (thickness: 30 nm) was fabricated on the ZnO substrate followed by stacking of the i-Si (thickness: 120 or 400 nm) and n-Si layers (thickness: 30 nm) with $T_p = 390$ °C, (3) the hydrogen-radical treatment was performed after fabricating the p-i-n structure, and (4) a 200-nm thick Al electrode with an area of $5 \times 5 \text{ mm}^2$ was deposited on the p-i-n structure by vacuum evaporation. We removed the silicon layers with a diamond pen to achieve contact with the ZnO electrode as shown in Figure 2.

Three types of solar cell (cell 1, cell 2, and cell 3) were fabricated by changing the thickness of the i-Si layer and dopant concentration of the p-Si layer, as listed in Table II. The dopant concentration was measured by SIMS.

For imaging the features of the p-i-n structure, the impurity distribution in the cell was examined by SIMS. Figure 3 shows the depth profiles for boron, phosphorus, zinc, carbon,

TABLE I. Properties of i-, p-, and n-Si films with and without the hydrogen-radical treatment.

| | i-Si | | p-Si ^a | | n-Si ^b | | i-Si (Ref) ^c |
|--|-----------------------|-----------------------|----------------------|----------------------|----------------------|----------------------|-------------------------|
| Hydrogen radical treatment | With | Without | With | Without | With | Without | Without |
| Hydrogen content (at. %) | 9.9 | 9.8 | 10.5 | 10.0 | 12.0 | 9.7 | 10 |
| Optical gap (eV) | 1.64 | 1.64 | 1.67 | 1.66 | 1.67 | 1.67 | 1.72 |
| Spin density (cm^{-3}) | $<2 \times 10^{16}$ | 5×10^{17} | 1×10^{17} | 6×10^{17} | 6×10^{16} | 4×10^{17} | $<2 \times 10^{16}$ |
| Photoconductivity (S/cm) ^d | 0.9×10^{-5} | 1.5×10^{-7} | ... | ... | ... | ... | 1.6×10^{-5} |
| Dark conductivity (S/cm) | 2.0×10^{-11} | 4.0×10^{-11} | 5.0×10^{-4} | 2.1×10^{-4} | 5.6×10^{-3} | 4.3×10^{-4} | 2.0×10^{-11} |

^aBoron concentration is $7 \times 10^{21} \text{ cm}^{-3}$.

^bPhosphorus concentration is $2 \times 10^{21} \text{ cm}^{-3}$.

^cPrepared by plasma-enhanced chemical vapour deposition method.

^dAM-1.5G solar simulator with an intensity of 100 mW/cm^2 was employed.

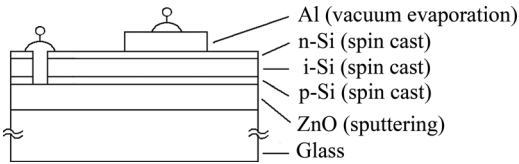


FIG. 2. Schematic of a solution-processed a-Si:H solar cell structure.

oxygen, and nitrogen for cell 1. The detection limits for boron, phosphorus, and zinc in Figure 3(a) are 2×10^{16} , 2×10^{18} , and $8 \times 10^{18} \text{ cm}^{-3}$, respectively. It can be observed that boron and phosphorus diffused in the i-Si layer, and the concentration of these species in the i-Si layer fell below the detection limit within 20–40 nm from each interface. We also confirmed that the boron diffuses extensively into the i-Si layer at $T_p > 390^\circ\text{C}$ (data not shown). Therefore, the upper limit of the fabrication temperature for the p-i-n structure with a satisfactory interface is 390°C . Although a low T_p is preferable to minimize the impurity diffusion, the lower limit of the fabrication temperature for obtaining a-Si:H layers was 360°C . The film oxidizes easily in the air at $T_p < 360^\circ\text{C}$ because the pyrolytic transformation of the polydihydrosilane into a-Si:H is not enough in low T_p . Figure 3(b) shows that carbon, oxygen, and nitrogen are distributed in the p-i-n structure with a concentration of 10^{19} – 10^{21} cm^{-3} , which increases at each interface. This concentration may be affected by the tools, the solvent, and the atmosphere in the glove box.

Figure 4 shows J–V characteristics at 25°C of the solution-processed solar cells with and without the hydrogen-radical treatment. The J–V curves denoted by c1, c2, and c3 (c'1, c'2, and c'3) correspond to cells 1, 2, and 3 with (without) the hydrogen-radical treatment, respectively. Moreover, photovoltaic parameters such as the open-circuit voltage (V_{oc}), short-circuit current (J_{sc}), fill factor (FF), and energy conversion efficiency (η) of cells 1, 2, and 3 as estimates from c1, c2, and c3 curves, respectively, are shown in the figure.

A comparison of c1–c3 with c'1–c'3 indicates that the hydrogen-radical treatment for the solution-processed solar cells significantly improved J_{sc} from $<0.2 \text{ mA/cm}^2$ to $>1.7 \text{ mA/cm}^2$. Accordingly, η improved from $<0.01\%$ to $>0.30\%$ for all cells. This enhancement in J_{sc} by the hydrogen-radical treatment may be because of the large improvement in photoconductivity for the i-Si layer, as shown in Table I. Therefore, we believe that the hydrogen-radical treatment is essential for the fabrication of solar cells using our solution-processed a-Si:H films.

TABLE II. Thickness and dopant concentrations of the p-, i-, and n-Si layers in cells 1, 2, and 3.

| | Cell 1 | Cell 2 | Cell 3 |
|--|------------------------------|------------------------------|------------------------------|
| n-Si: thickness (concentration) ^a | 30 nm (2×10^{21}) | 30 nm (2×10^{21}) | 30 nm (2×10^{21}) |
| i-Si: thickness | 120 nm | 120 nm | 400 nm |
| p-Si: thickness (concentration) ^a | 30 nm (7×10^{21}) | 30 nm (1×10^{21}) | 30 nm (7×10^{20}) |

^aUnit is in cm^{-3} .

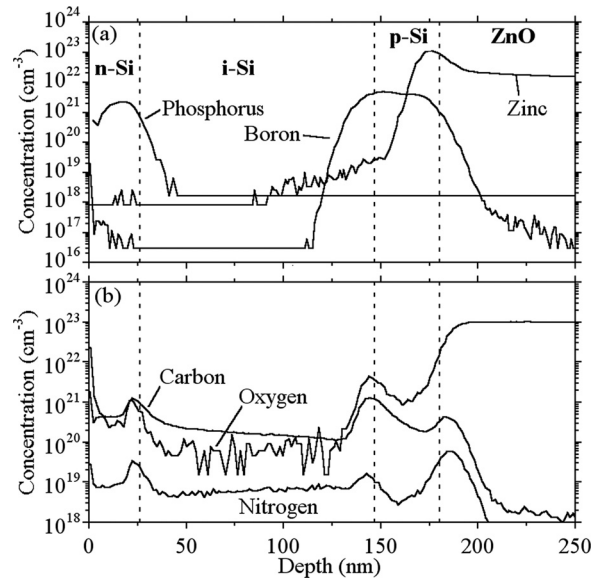


FIG. 3. Depth profiles of impurities in cell 1 measured by SIMS. (a) Boron, phosphorus, and zinc. (b) Carbon, oxygen, and nitrogen. $T_p = 390^\circ\text{C}$.

Regarding the photovoltaic parameters of the cells with the hydrogen-radical treatment, cell 3 shows the highest J_{sc} among all the cells and is characterised by low V_{oc} and the lowest values of FF among the cells. The highest J_{sc} for cell 3 with a thicker i-Si layer is supported by the largest number of photo-generated carriers in the i-Si layer compared with those of cells 1 and 2. The lowest FF value might result from the film quality of the i-Si layer, as shown in the micrographs of the i-Si surface for cell 1 (Figure 5(a)) and cell 3 (Figure 5(b)).

Cell 3 alone displayed a few cracks (arrows in Figure 5(b)) and asperity generated by large shrinkage, which is associated with pyrolysis of the thick (400 nm) i-Si layer. These defects may become a leakage current path and result in the decay of the insulation of the cell. Our experimental results suggest that the defect- and crack-free i-Si layers may improve the value of photovoltaic parameters. However, it was difficult to fabricate a thick film ($>300 \text{ nm}$) with high

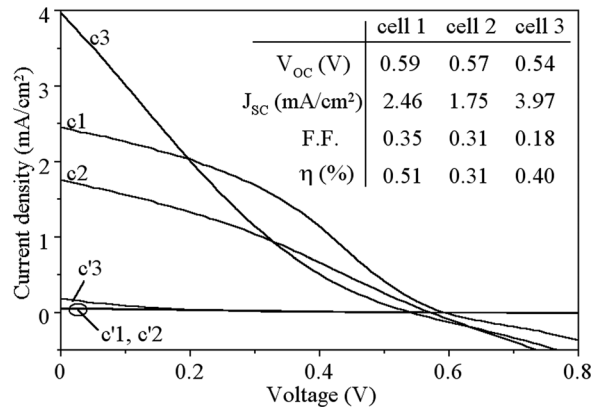


FIG. 4. J–V characteristics of the solar cells with the top electrode size of $5 \times 5 \text{ mm}^2$. The curves denoted by c1, c2, and c3 (c'1, c'2, and c'3) represent the J–V curves for cells 1, 2, and 3 with (without) the hydrogen-radical treatment, respectively. The inset shows the photovoltaic parameters and energy conversion efficiency for cells 1, 2, and 3 with the hydrogen-radical treatment. The curves were measured using the solar simulator under the illumination condition of AM-1.5G (100 mW/cm^2).

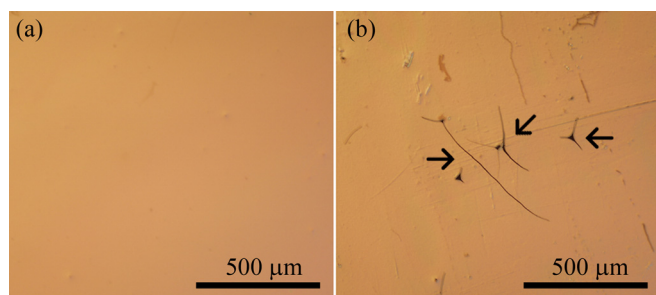


FIG. 5. Optical micrographs in the i-Si surface of (a) cell 1 and (b) cell 3.

uniformity and no cracks using the spin-cast method under the conditions employed at this time. Therefore, it is necessary when fabricating high-performance solution-processed solar cells to understand the liquid engineering principles for coating a thick film on a substrate and also to employ suitable coating techniques for a large substrate, such as an ink-jet or slit coating method.

In addition to improving the quality of thick i-Si layer, there are three problems still unsolved, which are as follows: (1) reduce the concentration of carbon, oxygen, and nitrogen (of the order of 10^{19} – 10^{21} cm $^{-3}$) causing the donor-like state,¹¹ (2) decrease the Schottky-barrier height at the p-Si/ZnO interface, which results in a large deviation from ideal J–V curves, and (3) remove native silicon oxide layers between each silicon layer, which acted as resistive components in the cells. We believe that increasing η can be achieved by overcoming these issues as well as preparing a high-quality thick i-Si layer.

In conclusion, we have fabricated a-Si:H p-i-n structure by employing a solution-based process using doped and non-doped polydihydrosilane solutions. Further, we have demonstrated the effectiveness of hydrogen-radical treatment for improving the conductivity of a-Si:H layers by a reduction in spin density. The solution-processed a-Si:H solar cells are shown to have η of 0.31%–0.51% under AM-1.5G (100 mW/cm 2) illumination. Even though η is low, the formation of the solution-processed silicon p-i-n structure indicates that the solution-based process might be a promising technology for future application to silicon devices. We also believe that the characteristics of our solar cells will be improved by optimization of processes and introducing the light-trapping structure.

¹J. Y. Kim, K. Lee, N. E. Coates, D. Moses, T. Q. Nguyen, M. Dante, and A. J. Heeger, *Science* **317**, 222 (2007).

²W. Wang, Y.-W. Su, and C.-H. Chang, *Sol. Energy Mater. Sol. Cells* **95**, 2616 (2011).

³T. Shimoda, Y. Matsuki, M. Furusawa, T. Aoki, I. Yudasaka, H. Tanaka, H. Iwasawa, D. Wang, M. Miyasaka, and Y. Takeuchi, *Nature (London)* **440**, 783 (2006).

⁴T. Masuda, Y. Matsuki, and T. Shimoda, *J. Colloid Interface Sci.* **340**, 298 (2009).

⁵T. Masuda, Y. Matsuki, and T. Shimoda, *Polymer* **53**, 2973 (2012).

⁶T. Masuda, Y. Matsuki, and T. Shimoda, *Thin Solid Films* **520**, 5091 (2012).

⁷H. Tanaka, H. Iwasawa, D. Wang, N. Toyoda, T. Aoki, I. Yudasaka, Y. Matsuki, T. Shimoda, and M. Furusawa, *Jpn. J. Appl. Phys.* **46**, L886 (2007).

⁸S. Kalbitzer, G. Muller, P. G. Le Comber, and W. E. Spear, *Philos. Mag. B* **41**, 439 (1980).

⁹A. Izumi and H. Matsumura, *Jpn. J. Appl. Phys.* **41**, 4639 (2002).

¹⁰*Thin-Film Silicon Solar Cells*, edited by A. Shah (EEPL, 2010), pp. 17–96.

¹¹T. Kinoshita, M. Isomura, Y. Hishikawa, and S. Tsuda, *Jpn. J. Appl. Phys.* **35**, 3819 (1996).